Structure of metastable states in spin glasses by means of a three replica potential

Andrea Cavagna, Irene Giardina, Giorgio Parisi

Dipartimento di Fisica

Università di Roma I, "La Sapienza"

P.le A. Moro 5, 00185 Roma, Italy

and

INFN Sezione di Roma I, Roma, Italy.

cavagna@roma1.infn.it

giardina@roma1.infn.it

parisi@roma1.infn.it

November 7, 1996

Abstract

In this paper we introduce a three replica potential useful to examine the structure of metastable states above the static transition temperature T_c, in the spherical p-spin model. Studying the minima of the potential we are able to find which is the distance between the nearest equilibrium and local equilibrium states, obtaining in this way information on the dynamics of the system. Furthermore, the analysis of the potential at the dynamical transition temperature T_d suggests that equilibrium states are not randomly distributed in the phase space.

1. Introduction.

In these years it has been realized that there are model systems for which the dynamics can be analytically studied in the infinite volume limit. In some of these systems, below a characteristic temperature T_d, called dynamical transition temperature, the phase space of the equilibrium configurations breaks down in regions (from here on valleys) where the system is trapped for an infinite time. Therefore, in this situation, if the system is near an equilibrium configuration at the initial time, it will remain in this region forever. The number of these regions is exponentially high as soon as $T > T_c$, where $T_c < T_d$ is the static transition temperature, at which only a finite number of valley starts to dominate the partition function; these features are clearly revealed by an analysis based on the TAP equations [1,2,3]. All the equilibrium valleys are characterized by the same energy density E, entropy density S_v and self-overlap q_{EA}. The total entropy density of the system will be given by

$$S = S_v + \Sigma \ , \tag{1.1}$$

where Σ is the so called configurational entropy or complexity, i.e. $\Sigma = (1/N) \ln \mathcal{N}$, where $\mathcal{N}$ is the exponentially high number of valleys and N is the size of the system. The complexity goes to zero at the transition temperature T_c.

It is also true that in the region $T < T_d$, if the system starts randomly at the initial time, the energy of the system evolves toward a value greater than the equilibrium one [2,4]. In other words, metastable states are present. In the rest of the paper these metastable states will be also called local equilibrium state, while the name equilibrium states will be reserved to valleys which have the correct equilibrium energy density.

It is clear that these features, especially the last one, are likely to be an artefact of the mean field approximation, which is correct in these models. It is therefore interesting to try to understand what happens when corrections to the mean field theory are present. The simplest case we can think about is when N is finite and large: the times to escape from a valley are likely to be exponentially high in N. The direct computation of these exponentially large times using the dynamical equations is rather involved and it has not been done. A partial solution to the problem consists in assuming the dynamics is dominated at ultra large times by the crossing of free energy barriers between different valleys and some information can thus be gathered by computing these barriers and by the analysis of the mutual disposition of metastable states.

This program cannot be pursued directly with the usual tools of statistical mechanics and we must resort to use a different method, the *real replica method* [2,5], in which two or more (in general M) real replicas are introduced. If we denote by $\mathbf{q}$ the $M \times M$ matrix of the overlaps imposed among the different real replicas

$$q_{a,b} = \frac{1}{N} \sum_i \sigma_i^a \sigma_i^b \ , \tag{1.2}$$

detailed information on the free energy landscape is carried by the free energy as function of $\mathbf{q}$. This program is quite recent. Up to this moment only the case $M = 2$ has been examined in details. In this case one computes a two replica potential $V_2(q_{12})$, which is the free energy of replica 2 constrained to have overlap q_{12} with replica 1, supposed to stay at equilibrium [5]. A different potential $W_{12}(q_{12})$ can be introduced, defined as the free energy increase of a pair of two replicas if we constrain them to stay at mutual overlap q_{12} [2]. The main difference among these two cases is the following:
In the first case replica 1 is at equilibrium and replica 2 is not, because it must satisfy a constraint; obviously for some particular values of q_{12} (e.g. $q_{12} = 0$) the constraint is harmless and also replica 2 is at equilibrium. In the second case replica 1 and 2 are chosen in such a way to satisfy a constraint and both will be in general out of equilibrium. The first construction is the most appropriate one if we want to get information on the free energy landscape around an equilibrium configuration. The relevant computations have been already done and they will be summarized here for reader convenience. From this two replica potential one can compute the dynamical transition and the configurational entropy, and obtain a first estimate of the barriers separating different valleys.

The question we address in this paper is the organization of equilibrium and local equilibrium states. For example, given a generic equilibrium configuration we would like to know which is the maximum overlap $\bar{q}$ at which is found a local equilibrium state.

In the same fashion we would like to know which is the maximum overlap $q^\star$ at which is found an equilibrium state. It is not evident *a priori* if $\bar{q} \neq q^\star$ (which is the result we find) or not.

In order to answer to this and other questions we need to consider a three replica potential $V_3(q_{12}, q_{13}, q_{23})$, which is the free energy of replica 3 constrained to stay at overlap q_{13} and q_{23} from replica 1 and replica 2 respectively, where replica 1 is an equilibrium configuration and replica 2 is constrained to stay at distance q_{12} from replica 1. This potential is useful to explore in more detail the free energy landscape with respect to the previous case where only two replicas are present. The stationary points of this potential correspond to local equilibrium states of the system.

In this paper we devote our attention to the p-spin spherical model, due to its simplicity and to the relatively simple form of the free energy. Similar considerations can be applied also to other models, but this will not be done in this paper. In Sect. 2 we recall for reader convenience the definition of the p-spin spherical model and the computation of the two replica potential. In Sect. 3 we present the computation for the three replica potential. The shape of the potential and its stationary points, which correspond to local equilibrium states, are computed in Sect. 4. In Sect. 5 we study the temperature dependence of the various quantities involved. Finally, in Sect. 6 we discuss some of the implications of our finding for the dynamics of the system at large volume. Two appendices contain the more technical aspects of the computations.

2. The two replica potential.

Let us introduce the p-spin spherical model [6,7,8,9], defined by the Hamiltonian

$$
\begin{gathered}
H(\sigma) = \sum_{i_1 < i_2 < \ldots < i_p} J_{i_1 \ldots i_p} \sigma_{i_1} \ldots \sigma_{i_p} \\
\frac{1}{N} \sum_i \sigma_i^2 = 1 \ ,
\end{gathered}
\tag{2.1}
$$

where the σ_i are real variables satisfying the spherical constraint; the couplings $J_{i_1 \ldots i_p}$ are independent Gaussian variables with variance

$$
\overline{J^2_{i_1 \ldots i_p}} = \frac{p!}{2N^{p-1}} \ . \tag{2.2}
$$

With these definitions

$$
\overline{H(\sigma) H(\sigma')} \stackrel{\text{def}}{=} N \frac{1}{2} f(q_{\sigma\sigma'}) = N \frac{1}{2} q^p_{\sigma\sigma'} \ , \tag{2.3}
$$

where $q_{\sigma\sigma'}$ is the overlap between the two configurations (see eq. (1.2)). We note that it is possible a generalization to random Hamiltonian models, specified by different forms of the correlation function f [10,11].

Following [5] we consider the two replica potential $V_2(q_{12})$, defined as the free energy cost to keep a configuration τ (replica 2) at a fixed overlap q_{12} with an equilibrium configuration σ (replica 1):

$$
-\beta N V_2(q_{12}) = -\beta N (F_{fixed} - F_{free}) =
$$

$$
\overline{\frac{1}{Z_{free}} \int d\sigma \exp(-\beta H(\sigma)) \ \log \left(\int d\tau \exp(-\beta H(\tau)) \ \delta(q_{\sigma\tau} - q_{12}) \right)} - \overline{\log Z_{free}} \ . \tag{2.4}
$$

It is important to note that in this way we compute the free energy only of the second replica τ, while we operate an annealed average over σ. Indeed, this can be done by virtue of the assumption that the constrained free energy F_{fixed} is self-averaging with respect to σ. To perform the average on the quenched disorder, we use the replica trick:

$$-\beta N V_2(q_{12}) =$$

$$= \lim_{n,m\to 0} \frac{1}{m} \log \overline{\int d\sigma_a d\tau_b \exp\left[-\beta\left(\sum_{a=1}^{n} H(\sigma_a) + \sum_{b=1}^{m} H(\tau_b)\right)\right] \prod_{b=1}^{m} \delta(q_{\sigma_1 \tau_b} - q_{12})} \tag{2.5}$$

$$- \overline{\log Z_{free}} \ .$$

We introduce the overlap sub-matrices

$$\begin{aligned} Q^{11}_{ab} &= q_{\sigma_a \sigma_b} \qquad a = 1, \dots, n;\ b = 1, \dots, n \\ Q^{12}_{ab} &= q_{\sigma_a \tau_b} \qquad a = 1, \dots, n;\ b = 1, \dots, m \\ Q^{22}_{ab} &= q_{\tau_a \tau_b} \qquad a = 1, \dots, m;\ b = 1, \dots, m \ ; \end{aligned} \tag{2.6}$$

and the total matrix of the overlap $\mathbf{Q}$, formed by the blocks (2.6). With this definition, equation (2.5) gives

$$-\beta V_2(q_{12}) = \lim_{n,m\to 0} \frac{1}{2m} \left(\beta^2 \sum_{a,b} f(\mathbf{Q}_{ab}) + \log\det \mathbf{Q} \right) + \beta F_{free} \ . \tag{2.7}$$

Before proceeding with the calculation, it is necessary to give sensible ansatz for the overlap sub-matrices. From now on we will consider only temperatures T greater than T_c and zero external magnetic field; therefore, since Q^{11} is referred to an independent free system, we assume for it the symmetric form

$$Q^{11}_{ab} = \delta_{ab} \ . \tag{2.8}$$

The structure of Q^{12} is in part imposed by the constraint in (2.5), that forces the first row to be equal to q_{12}. The simplest ansatz for the whole matrix is

$$Q^{12}_{ab} = q_{12}\ \delta_{a,1} \ . \tag{2.9}$$

This choice is confirmed by the analysis of the potential in the limit[1] $\beta \to 0$; moreover, if we introduce an additional parameter w_{12} for the rest of the matrix, the saddle point equations lead to the solution $w_{12} = 0$.

[1] At β=0 the calculation reduces to a purely geometrical problem; indeed, in this case the potential is simply proportional to the volume of the phase space region accessible to the constrained replica. Therefore, the comparison with this limit is crucial to test the ansatz for the overlap matrices.

In [5] Q^{22} was assumed symmetric, but a successive examination suggested that a more general one step RSB form has to be taken [12], with variational parameters (x_r, r_1, r_0):

$$Q^{22}_{ab} = (1-r_1)\delta_{ab} + (r_1 - r_0)\epsilon_{ab} + r_0 \ , \tag{2.10}$$

where ϵ_{ab} is equal to one in the diagonal blocks of size x_r and zero elsewhere.

With these assumptions we obtain (see Appendix A for details):

$$\begin{aligned} -2\beta V_2(q_{12}) = {} & 2\beta^2 f(q_{12}) + \beta^2(x_r-1)f(r_1) - \beta^2 x_r f(r_0) \\ & + \log(1-r_1) + \frac{1}{x_r}\log\left(1 + x_r\frac{r_1-r_0}{1-r_1}\right) + \frac{r_0 - q_{12}^2}{1-r_1+x_r(r_1-r_0)} \ . \end{aligned} \tag{2.11}$$

The parameters with respect to which the potential has to be maximized are (x_r, r_1, r_0) and the saddle point equations read:

$$\begin{aligned} (1-x_r)\beta^2 f'(r_1) &= (1-x_r)\ \frac{1}{(1-r_1+x_r(r_1-r_0))^2}\left(r_1 - q_{12}^2 + x_r\frac{(r_1-r_0)^2}{1-r_1}\right) \\ x_r\beta^2 f'(r_0) &= x_r\ \frac{(r_0-q_{12}^2)}{(1-r_1+x_r(r_1-r_0))^2} \\ \beta^2 f(r_1) - \beta^2 f(r_0) &= \frac{1}{x_r^2}\log\left(1+x_r\frac{r_1-r_0}{1-r_1}\right) \\ & \qquad - \frac{1}{x_r}(r_1-r_0)\ \frac{1-r_1+x_r(r_1-2r_0+q_{12}^2)}{(1-r_1+x_r(r_1-r_0))^2} \ . \end{aligned} \tag{2.12}$$

Setting $r_0 = r_1$ we obviously recover the replica symmetric expressions given in [5].

The RSB ansatz for Q^{22} slightly modifies the shape of the potential V_2 (see Fig. 1) eliminating the secondary minimum found in [5], the interpretation of which was unclear. For the rest, all the features of the potential remain the same: there is an absolute minimum for $q_{12} = 0$ with $V_2 = 0$, which represents a typical equilibrium configuration of the second replica τ; moreover for $T < T_d$ there is a relative minimum M for $q_{12} = q_{EA}$ corresponding to the situation in which τ is in the same pure state as the first replica σ. We note that in this second situation, the configuration τ is of equilibrium but not typical, in the sense that, for entropic reasons, if the system were not constrained, it would be very unlikely to find τ in the same pure state of σ. It turns out that the value of the potential in M gives information on the number of dominant pure states, i.e.

$$V_2(q_{EA}) = T\Sigma \ , \tag{2.13}$$

where Σ is the configurational entropy [5].

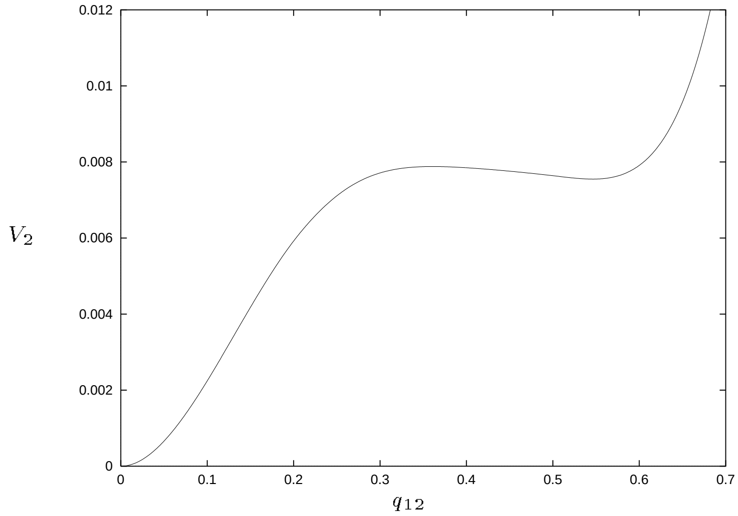

Fig. 1: The potential V_2 at β=1.64 and p=3; q_{EA}=0.546.

3. The three replica potential.

As we have seen, the analysis of V_2 gives information on the self-overlap and on the number of the states dominating at a certain temperature. It remains rather unclear how the phase space is organized in terms of these states; in other words, we would like to know more about their mutual overlaps, and study the evolution of the whole structure with the temperature.

A natural generalization of the method that leads to V_2, consists in considering three different real replicas, constrained to have fixed mutual overlap, as we are going to explain. As in the case of V_2, we take a first independent replica ρ which thermalizes freely at a temperature T. We then consider a second replica σ constrained to thermalize at a fixed overlap q_{12} with ρ. Finally, we calculate the free energy of a third replica τ constrained to have overlap q_{13} with ρ and q_{23} with σ. In this way it is possible to define a three replica potential V_3, taking the difference between the constrained free energy of τ and the free energy of the unconstrained system:

$$
\begin{aligned}
&-\beta N V_3(q_{12}, q_{13}, q_{23}) = \\
&= \overline{\frac{1}{Z_{free}} \int d\rho \exp(-\beta H(\rho)) \frac{1}{Z(\rho; q_{12})} \int d\sigma \exp(-\beta H(\sigma))\ \delta(q_{\rho\sigma} - q_{12}) \times} \\
&\quad \overline{\log \int d\tau \exp(-\beta H(\tau))\ \delta(q_{\rho\tau} - q_{13})\ \delta(q_{\sigma\tau} - q_{23})} - \overline{\log Z_{free}}\ ,
\end{aligned}
\tag{3.1}
$$

with

$$
Z(\rho; q_{12}) = \int d\sigma \exp(-\beta H(\sigma))\ \delta(q_{\rho\sigma} - q_{12})\ . \tag{3.2}
$$

In our analysis we limit ourselves to the situation in which the temperatures are the same for the three replicas. Our purpose is to study the potential V_3 in the plane (q_{13}, q_{23}) at various fixed values of q_{12}. In this way, through the position of replica 3, we can explore the neighborhood of replica 2, which is not a configuration of equilibrium for the free system; this is possible because of the different role of the first and second replica. By the usual trick we get

$$
\begin{aligned}
&-\beta N V_3(q_{12}, q_{13}, q_{23}) = \\
&= \lim_{n,m,l\to 0} \frac{1}{l} \log \overline{\int d\rho_a d\sigma_b d\tau_c \exp\left[-\beta\left(\sum_{a=1}^{n} H(\rho_a) + \sum_{b=1}^{m} H(\sigma_b) + \sum_{c=1}^{l} H(\tau_c)\right)\right] \times} \\
&\quad \overline{\prod_{b=1}^{m} \delta(q_{\rho_1\sigma_b} - q_{12}) \prod_{c=1}^{l} \delta(q_{\rho_1\tau_c} - q_{13})\delta(q_{\sigma_1\tau_c} - q_{23})} - \overline{\log Z_{free}}\ .
\end{aligned}
\tag{3.3}
$$

Again we introduce the sub-matrices:

$$
\begin{aligned}
Q^{11}_{ab} &= q_{\rho_a\rho_b} \qquad a = 1,\ldots,n;\ b = 1,\ldots,n \\
Q^{12}_{ab} &= q_{\rho_a\sigma_b} \qquad a = 1,\ldots,n;\ b = 1,\ldots,m \\
Q^{22}_{ab} &= q_{\sigma_a\sigma_b} \qquad a = 1,\ldots,m;\ b = 1,\ldots,m \\
Q^{13}_{ab} &= q_{\rho_a\tau_b} \qquad a = 1,\ldots,n;\ b = 1,\ldots,l \\
Q^{23}_{ab} &= q_{\sigma_a\tau_b} \qquad a = 1,\ldots,m;\ b = 1,\ldots,l \\
Q^{33}_{ab} &= q_{\tau_a\tau_b} \qquad a = 1,\ldots,l;\ b = 1,\ldots,l\ ;
\end{aligned}
\tag{3.4}
$$

and the total overlap matrix $\mathbf{Q}$. In analogy with the case of V_2, the expression of V_3 in terms of $\mathbf{Q}$ after averaging over the disorder, is

$$-\beta V_3(q_{12},q_{13},q_{23}) = \lim_{n,m,l\to 0} \frac{1}{2l}\left(\beta^2 \sum_{a,b} f(\mathbf{Q}_{ab}) + \log\det\mathbf{Q}\right) + \beta F_{free} \ . \tag{3.5}$$

It is important to bear in mind the difference between the roles of replicas 1 and 2, which is encoded in the different form of the relative overlap matrices. Q^{11} refers to the first free replica, while Q^{22} refers to replica 2, which thermalizes at *fixed* overlap q_{12} with 1. Both replicas are however independent from the third one, so the form of Q^{11}, Q^{12} and Q^{22} is identical to the one assumed in the case of V_2 and the value of the variational parameters (x_r, r_1, r_0), which are function of q_{12}, are determined by the same equations (2.12).

In second place, Q^{33} is assumed one step RSB, with parameters (x_s, s_1, s_0):

$$Q^{33}_{ab} = (1-s_1)\delta_{ab} + (s_1 - s_0)\epsilon_{ab} + s_0 \ ; \tag{3.6}$$

there is no reason to set $x_s = x_r$, since just as Q^{22} is broken independently from Q^{11}, the breakings of Q^{22} and Q^{33} have to be assumed independent; moreover, there are no algebraic motivations for this equality.

For what concerns Q^{13}, the limit $\beta \to 0$ shows that it is correct to assume a form similar to Q^{12},

$$Q^{13}_{ab} = q_{13}\ \delta_{a,1} \ . \tag{3.7}$$

However, the same limit shows that this form is no longer valid for Q^{23}; namely, the first row will still be equal to q_{23}, but the rest of the matrix no more can be set equal to zero. Moreover, the structure of Q^{23} has to take into account the RSB form of Q^{22}: if replicas 2 are organized into clusters, it can be that the overlap of 3 with the particular cluster that contains the *first* replica σ_1 of 2 (this is the only replica of 2 *really* coupled to 3, as shown in (3.3)) is different from the overlap of 3 with any other cluster.

Therefore, we postulate a RSB form also for Q^{23}. This is possible if we break the symmetry in the rows of Q^{23} in the following way:

$$Q^{23}_{ab} = (q_{23} - w_{23})\delta_{a,1} + (w_{23} - z_{23})\epsilon_{a,1} + z_{23} \ . \tag{3.8}$$

This one step RSB needs a breaking point x, but the genesis of the breaking shows clearly that for Q^{23} it has to be taken as breaking point x_r, that is the same of Q^{22}.

In conclusion, the new variational parameters are:

$$x_s, s_1, s_0, w_{23}, z_{23} \ . \tag{3.9}$$

With these ansatz, the expression of V_3 is (see Appendix B for details)

$$\begin{aligned} -2\beta V_3(q_{12}, q_{13}, q_{23}) = & \ 2\beta^2 f(q_{13}) + 2\beta^2 f(q_{23}) + 2\beta^2 (x_r - 1) f(w_{23}) - 2\beta^2 x_r f(z_{23}) \\ & + \beta^2 (x_s - 1) f(s_1) - \beta^2 x_s f(s_0) \\ & + \log(1 - s_1) + \frac{1}{x_s} \log\left(1 + x_s \frac{s_1 - s_0}{1 - s_1}\right) + \frac{s_0 - y}{1 - s_1 + x_s(s_1 - s_0)} \ , \end{aligned} \tag{3.10}$$

with

$$\begin{aligned} y = q_{13}^2 & + (q_{23} - w_{23})^2 (a + b + c) + 2(q_{23} - w_{23})(w_{23} - z_{23})(a + x_r(b + c)) \\ & + 2(q_{23} - w_{23})(z_{23} - q_{12} q_{13})(a + b x_r) + (w_{23} - z_{23})^2 x_r (a + x_r(b + c)) \\ & + 2(w_{23} - z_{23})(z_{23} - q_{12} q_{13}) x_r (a + b x_r) \ , \end{aligned} \tag{3.11}$$

and

$$\begin{aligned} a &= \frac{1}{1 - r_1} \\ b &= - \frac{r_1 - r_0}{1 - r_1} \cdot \frac{1}{1 - r_1 + x_r(r_1 - r_0)} \\ c &= - \frac{r_0 - q_{12}^2}{(1 - r_1 + x_r(r_1 - r_0))^2} \ . \end{aligned} \tag{3.12}$$

Expression (3.10) is very similar to the one of $V_2(q_{12})$ with (x_s, s_1, s_0) playing the role of (x_r, r_1, r_0) and y instead of q_{12}^2. Indeed, the saddle point equations for (x_s, s_1, s_0) are in form exactly identical to (2.12), changing q_{12}^2 into y. Moreover, V_3 has to be maximized with respect to w_{23} and z_{23}:

$$\begin{aligned} (1 - x_r)\beta^2 f'(w_{23}) = & \ (1 - x_r) \ \frac{1}{1 - s_1 + x_s(s_1 - s_0)} [(q_{23} - w_{23})(b + c) \\ & + (w_{23} - z_{23})(a + x_r(b + c)) + (z_{23} - q_{12} q_{13})(a + b x_r)] \\ x_r \beta^2 f'(z_{23}) = & \ x_r \ \frac{1}{1 - s_1 + x_s(s_1 - s_0)} [(q_{23} - w_{23}) c \\ & + x_r (w_{23} - z_{23}) c + (z_{23} - q_{12} q_{13})(a + b x_r)] \ . \end{aligned} \tag{3.13}$$

We note that the equations for (x_s, s_1, s_0) are coupled to equations (3.13) by means of y, that contains w_{23} and z_{23}.

Let us now examine under which conditions the case of V_2 is recovered. It turns out that

$$\begin{aligned} V_3(q_{12}=0, q_{13}=0, q_{23}) &= V_2(q_{23}) \\ V_3(q_{12}=0, q_{13}, q_{23}=0) &= V_2(q_{13}) \ . \end{aligned} \tag{3.14}$$

This is just what we expected for the following reason: setting $q_{12} = 0$ replica 2 thermalizes as in the free case and so replica 1 and 2 are both equilibrium configurations. In this situation, if we set, for example, $q_{13} = 0$, the constraint 1-3 is harmless and the pair 2-3 reproduces the case of V_2; the same is true for $q_{23} = 0$.

4. The shape of the potential.

The most important information in the study of V_3 comes from the analysis of its minima in the plane (q_{13}, q_{23}) at fixed values of q_{12}, which correspond to stable or metastable states of the system. We then minimize V_3 with respect of q_{13} and q_{23}:

$$\begin{aligned} \beta^2 f'(q_{13}) =& \frac{1}{1-s_1+x_s(s_1-s_0)}[q_{13} - q_{12}(q_{23}-w_{23})(a+bx_r) \\ & - q_{12}(w_{23}-z_{23})x_r(a+bx_r)] \\ \beta^2 f'(q_{23}) =& \frac{1}{1-s_1+x_s(s_1-s_0)}[(q_{23}-w_{23})(a+b+c) \\ & + (w_{23}-z_{23})(a+x_r(b+c)) + (z_{23}-q_{12}q_{13})(a+bx_r)] \ . \end{aligned} \tag{4.1}$$

First of all, we note that for each value of q_{12} there is a solution of (4.1) for $q_{13} = q_{23} = 0$, with $V_3 = 0$. This is the absolute minimum of the potential in the (q_{13}, q_{23}) plane and corresponds to the situation in which the third replica sees a phase space identical to that of the unconstrained system[2].

[2] The requirement that replica 3 is sited somewhere in the phase space, translates into the formula: $\int dq_{13} dq_{23} e^{-NV_3(q_{13},q_{23})} = 1 \quad \forall q_{12}$, and for $N \to \infty$ this implies that in the absolute minimum the potential has to be zero, as it is in our case.

For what concerns non trivial minima, the numerical analysis of equations (4.1) in the case $p = 3$, shows the following pattern:

i) For any value of q_{12} and for any temperature in the range (T_c, T_d), we find a minimum M_1 with

$$\begin{aligned} q_{13} &= q_{EA} \\ q_{23} &\sim q_{12} \\ V_3(M_1) &= V_2(q_{EA}) \ . \end{aligned} \tag{4.2}$$

The interpretation of M_1 is very simple: the third replica is in the same pure state of the first one, independently from the value of q_{12}; M_1 has exactly the same meaning of M for the two replica potential. As q_{12} grows, the second replica approaches this state, not changing the potential, until for $q_{12} = q_{EA}$ the three replicas are all in the same state and $q_{12} = q_{13} = q_{23} = q_{EA}$. We call this point Ω.

It is important to note that $q_{23} = q_{12}$ holds only in three points (see Fig. 2). Obviously it happens for $q_{12} = 0$. Then, as q_{12} grows, we have $q_{12} > q_{23}$ and this holds until $q_{12} = q_{max}$, where q_{max} is the value for which V_2 has its maximum; here again $q_{12} = q_{23}$. For $q_{max} < q_{12} < q_{EA}$ we have the opposite situation, with $q_{12} < q_{23}$, until we reach Ω.

This behaviour is consistent with the idea that at a distance q_{max} from the state of replica 1 the free energy reaches a maximum; the interpretation of Fig. 2 is then the following: Replicas 1 and 3 are in the same state but they have not the same role: replica 1 is some quenched typical configuration of the state, while, in some sense, replica 3 represents the center of the state, because of the thermodynamic average. When $q_{12} < q_{max}$, replica 2 reaches its minimum energy taking the maximum distance from the center of the state, compatibly with the given value of q_{12}, and in so doing q_{23} results lower than q_{12}. The opposite situation holds when $q_{12} > q_{max}$.

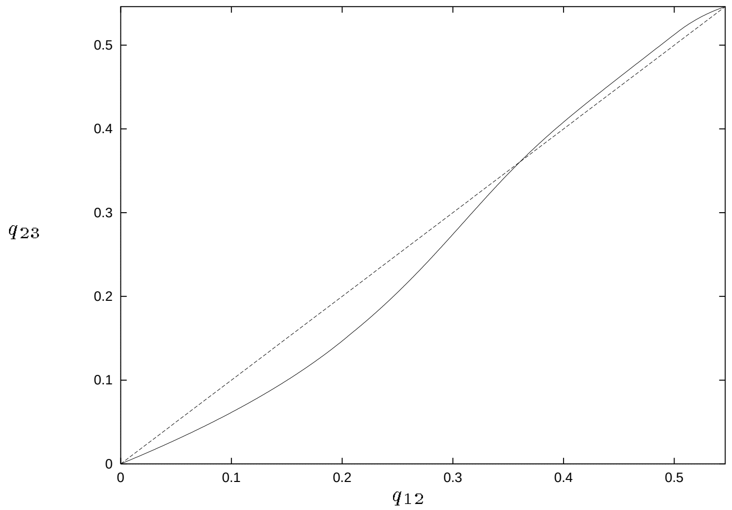

Fig. 2: q_{23} in M_1 as a function of q_{12} at β=1.64; q_{max}=0.361, q_{EA}=0.546.

ii) More interesting is the presence of a minimum with the third replica close to the second one. For T in the usual range (T_c, T_d) and $0 \leq q_{12} \leq \bar{q}(T)$ we find a minimum M_2 with

$$\begin{aligned} &q_{23} \sim q_{EA} \\ &q_{13} \sim q_{12} \leq \; q_{EA} \; . \end{aligned} \tag{4.3}$$

It is important to note that the last value $\bar{q}$ of q_{12} for which M_2 exists is at any temperature less or equal to q_{EA}.

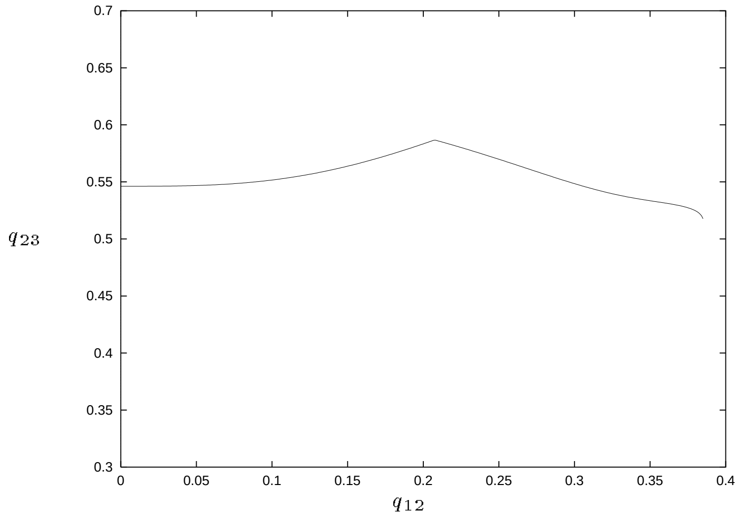

Fig. 3a: q_{23} in M_2 as a function of q_{12} at β=1.64; q_{EA}=0.546, $\bar{q}$=0.385.

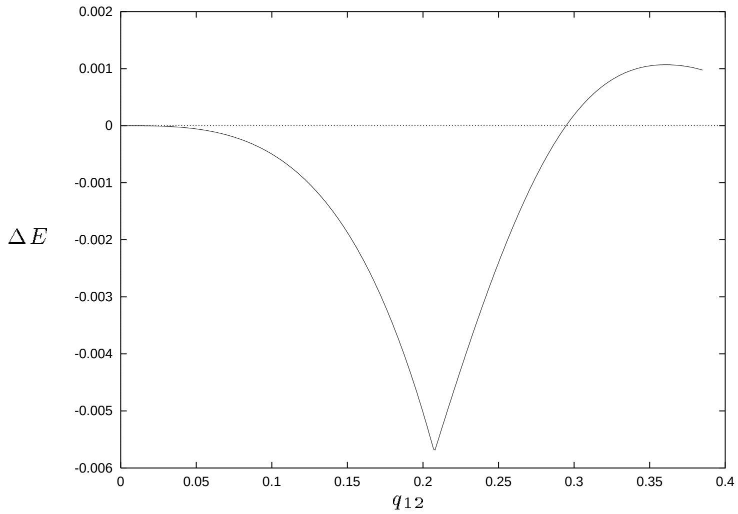

Fig. 3b: The energy difference ΔE in M_2 as a function of q_{12} at β=1.64; $q^\star$=0.295, $\bar{q}$=0.385.

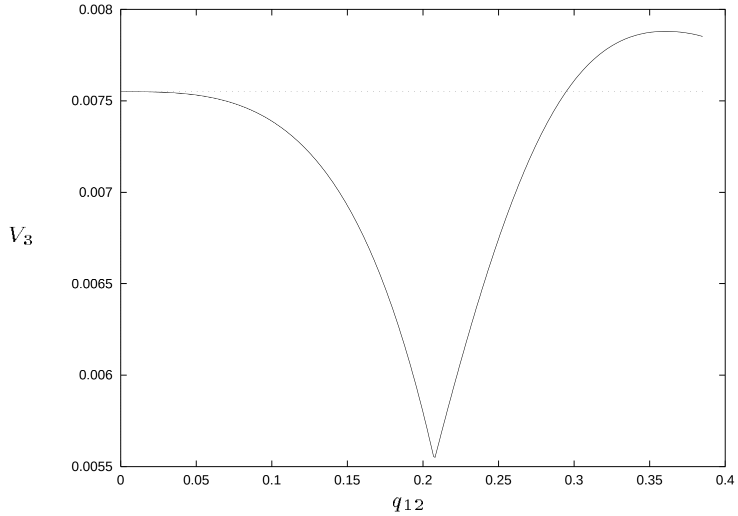

Fig. 3c: The potential V_3 in M_2 as a function of q_{12} at β=1.64; $q^\star$=0.295, $\bar{q}$=0.385.

Let us fix a reference temperature T and examine M_2 at different values of q_{12}. For $q_{12} = 0$ we have $q_{13} = 0$, $q_{23} = q_{EA}$ and $V_3(M_2) = V_2(q_{EA})$; this is trivial because we have seen that in this case V_3 reduces to V_2. When $q_{12} \neq 0$ we force the second replica to thermalize in a restricted portion of the phase space; the fact that we still find the minimum M_2 corresponding to the third replica in equilibrium close to the second one, shows that there are local equilibrium states even at non zero overlap q_{12} with the state of the first free replica. The variation with q_{12} of the interesting quantities evaluated in

M_2 is shown in Fig. 3.

We note that q_{23} remains close to q_{EA}, confirming the hypothesis that the second and the third replica are in the same state. It is then crucial to verify if the states corresponding to the minima M_2 can be identified with TAP solutions, i.e. if their free energy and self-overlap satisfy the TAP equations. First, at fixed q_{12}, the self-overlap of the state relative to M_2 is given by s_1 (see eq.(3.6)). Secondly, we must compute the free energy of this particular state; to this end we can write

$$V_3(M_2) = (f_3 - T\Sigma_3) - F_{free} \ , \tag{4.4}$$

where f_3 is the free energy of the state in which replica 3 thermalizes, and Σ_3 is the logarithm of the number of states accessible to replica 3, compatibly with the constraints; obviously, since replica 3 is in the same state of replica 2, which is fixed, we have $\Sigma_3 = 0$ and therefore

$$f_3 = V_3(M_2) + F_{free} \ . \tag{4.5}$$

It turns out that in M_2 the relation holding between f_3 and s_1 is always the same of the TAP approach [2]. In other words, the state corresponding to M_2 coincides with that particular TAP solution specified by

$$\begin{aligned} f_{TAP} &= f_3 \\ q_{TAP} &= s_1 \ . \end{aligned} \tag{4.6}$$

Let us now consider the behaviour in M_2 of the energy difference $\Delta E = E - E_{free}$: we note that there is a value $q_{12} = q^\star$ for which

$$\Delta E(q^\star) = \ 0 \ . \tag{4.7}$$

The fact that in this minimum the energy is equal to the one of the unconstrained system means that replicas 2 and 3 are in a state of the same kind of the one chosen by the unconstrained system, that is one of the TAP solutions dominating the equilibrium; indeed, we have $s_1(q^\star) = q_{EA}$ (the same happens in the minimum M of V_2). For this reason, the valley entropic contribution S_v to V_3 is the same as in the free case (see eq.(1.1)). Thus we expect

$$V_3(q^\star) = T\Sigma = V_2(q_{EA}) \ , \tag{4.8}$$

that is what we find (see Fig. 3c).

Therefore, we have the following picture: at temperature T with $T_c < T < T_d$, there is an exponentially high number of equilibrium states partitioning the phase space and the first unconstrained replica will thermalize into one of them, call it K. From our discussion follows that the closest states of the same kind and with the same energy density of K, are found at overlap $q^\star$ with K. Moreover, the fact that the last minimum M_2 is found at $q_{12} = \bar{q}$, shows that at smaller distances there are local equilibrium states with higher energy density, the closest of which have overlap $\bar{q}$ with K.

5. Temperature dependence.

Up to this moment we have studied V_3 at fixed temperature; now we examine the evolution of the system with T, in particular in the two limits $T \to T_c$ and $T \to T_d$.

At T_c the configurational entropy Σ of the dominant equilibrium states goes to zero [2,3]; this means that the number of these states becomes of order N and they *all* have zero overlap with each other. In this situation we expect that, fixed an equilibrium state, the closest one is at overlap zero; indeed, we find that $q^\star \to 0$ for $T \to T_c$. On the other side, at T_c the equilibrium states have the lowest energy density [2,3], while there is an exponentially high number of local equilibrium states with higher energy; according to this we find a non zero value of $\bar{q}$ even at T_c.

What happens at T_d is more interesting. First, we know that at this temperature the equilibrium states have the highest energy density, so we expect not to find local equilibrium states at higher energy; this is exactly what we have, since $\bar{q} \to q^\star$ for $T \to T_d$. Moreover, at this temperature Σ reaches a finite value, meaning that the number of the equilibrium states is still exponentially high; therefore, it is not clear *a priori* what is their minimum mutual distance. The very interesting feature shown by our potential is that

$$\bar{q}, q^\star \to q_d \quad \text{for} \quad T \to T_d \ , \tag{5.1}$$

where q_d is the value of q_{EA} at the dynamical transition. Equation (5.1) means that as T approaches T_d, the closest equilibrium states collapse into a single state of self-overlap q_d.

More precisely, for $T \sim T_d$ and $p = 3$, we find

$$\begin{aligned} q_{EA} &= (T_d - T)^{1/2} + q_d \quad , \quad q_d = 0.5 \\ q^\star &= a\ (T_d - T)^b + c \ . \end{aligned} \tag{5.2}$$

A fit of the numerical data gives

$$\begin{aligned} a &= -1.2 \\ b &= 0.24 \\ c &= 0.5004 \ . \end{aligned} \tag{5.3}$$

As we have seen, this indicates that $q^\star$ reaches q_d at T_d. The value of the exponent b can be less firmly established; indeed, if we make a fit fixing $c = 0.5$ we get

$$b = 0.30 \ . \tag{5.4}$$

Finally, we can study the potential for $T > T_d$. In this range the dominant equilibrium state is the paramagnetic one and the two replica potential has just the minimum in zero; for this reason the minimum M_1 of V_3 disappears, and do not exist other minima with $\Delta E = 0$. However we still find the minimum M_2 in a restricted range of q_{12} (see Fig. 4), to point out the existence of local equilibrium states even at temperature greater than T_d, corresponding to TAP solutions surviving above T_d. This situation holds up to a temperature $T_{last} > T_d$ over which all non trivial minima disappear. For $p = 3$ we have

$$\begin{aligned} \beta_c &= 1.706 \\ \beta_d &= 1.633 \\ \beta_{last} &= 1.573 \ . \end{aligned} \tag{5.5}$$

With regard to this see also [13].

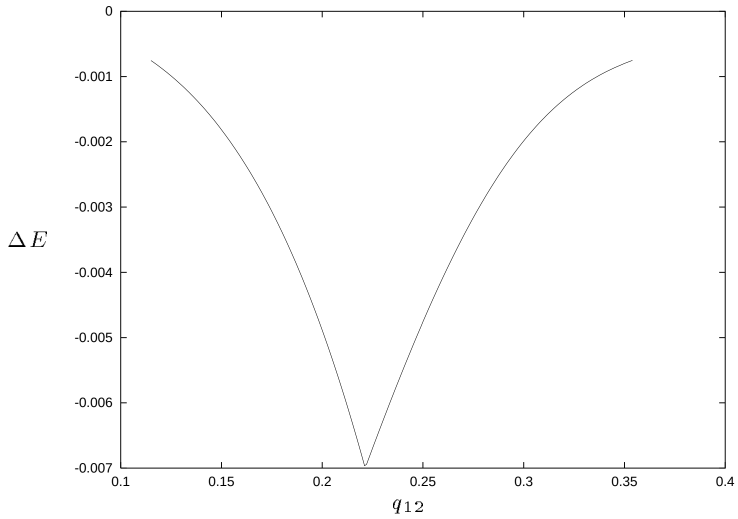

Fig. 4: The energy difference ΔE in M_2 as a function of q_{12} at $\beta<\beta_d$.

6. Open questions and hints on the dynamics.

Let us summarize some of our findings which are relevant for studying the dynamics. Near each equilibrium valley there are local equilibrium states with energy density greater that the equilibrium one. These local equilibrium states do exist up to a value $\bar{q}$ of the overlap, while the nearest equilibrium states are found at overlap $q^\star$. At the dynamical transition the three values $\bar{q}$, $q^\star$ and q_d merge.

The most surprising consequence of this picture is that the equilibrium states are not uncorrelated, i.e. they are not distributed randomly on the sphere, which would be the simplest possibility. Indeed, if they were randomly distributed, the nearest ones would be always at an overlap q, given by

$$\ln\left(1-\frac{q^2}{q_{EA}^2(T)}\right) = -2\Sigma(T) \ , \tag{6.1}$$

which should remain definitively different from q_d when $T\to T_d$, since $\Sigma(T_d)$ has a finite value.

It seems that the equilibrium valley, that at T_d has a flat direction (the replicon eigenvalue is zero), bifurcates in a bunch of not too different valleys below T_d, like in the SK model. However, the organization of equilibrium states is not the same as in the SK model, because it shows up only when we add a constraint to the system. It may be possible, as suggested in [14], that this situation may be in some way described by a non-monotonous function $q(x)$, as for example the one found in [2,15].

We can now ask what happens to a configuration starting at time zero near an equilibrium one. In particular we are interested to compute the typical behaviour of the overlap $q(t)$ among the configuration at time zero and the configuration at time t. It is natural to suppose that the form of the function $q(t)$ will be typical of a punctuated equilibrium: exponentially long period of stasis, where $q(t)$ fluctuates around a value that corresponds to a local equilibrium state, punctuated with fast variations of $q(t)$, which correspond to jumps between one local equilibrium and other local equilibrium states.

According to the previous picture the following scenario is rather likely. After a short transient time $q(t)$ will go to a value equal to the self-overlap of the valley, i.e. q_{EA}. After some exponentially large time it will jump to one of the nearest equilibrium states. If the barriers increase with increasing the distance (and therefore with decreasing the overlap) the most likely situation consists of a jumping to a local equilibrium state with overlap $\bar{q}$.

What happens at later times is not clear. If the different local equilibrium states are not correlated among themselves, (many replica potential is needed to investigate this point further), the system will return to the original state after some exponentially large time. Only after many attempts the system will jump to another equilibrium state at distance $q^\star$. At this point the system will not likely jump back and it will start from this point to do further jumps.

The scenario we have presented here seems to be the simplest one compatible with our finding on the three replica potential. In a future paper we plan to compare this proposal with numerical simulations. It would also be interesting to study the problem in the Random Energy Model, where many detailed computations can be done.

Acknowledgments.

It is a pleasure to thank Silvio Franz for very useful suggestions and discussion.

Appendix A.

In this appendix we calculate explicitly the final form of the potential $V_2(q_{12})$. We have:

$$-\beta V_2(q_{12}) = \lim_{n,m\to 0} \frac{1}{2m} \left(\beta^2 \sum_{a,b} f(\mathbf{Q}_{ab}) + \log\det \mathbf{Q} \right) + \beta F_{free} \ . \qquad \text{(A.1)}$$

This expression has to be computed according to the particular form assumed for the overlap matrix. The first part is

$$\lim_{n,m\to 0} \frac{1}{m} \beta^2 \sum_{ab} f(\mathbf{Q}_{ab}) =$$

$$2\beta^2 f(q_{12}) + \beta^2 f(1) + \beta^2 (x_r - 1) f(r_1) - \beta^2 x_r f(r_0) \ . \qquad \text{(A.2)}$$

The second part is the most complicated one. It is useful to exploit the following relation:

$$\log\det \mathbf{Q} = \log\det Q^{11} + \log\det \left(Q^{22} - Q^{21} (Q^{11})^{-1} Q^{12} \right) \ , \qquad \text{(A.3)}$$

where Q^{21} stands for $(Q^{12})^T$. With our ansatz, from (2.8) and (2.9)

$$\log\det Q^{11} = 0 \ , \qquad \text{(A.4)}$$

and

$$Q^{21} (Q^{11})^{-1} Q^{12} = q_{12}^2 \ , \qquad \text{(A.5)}$$

is a constant matrix. In this way equation (A.3) becomes

$$\log\det \mathbf{Q} = \log\det R \ , \tag{A.6}$$

with

$$R_{ab} = Q^{22}_{ab} - q^2_{12} = (1-r_1)\delta_{ab} + (r_1 - r_0)\epsilon_{ab} + (r_0 - q^2_{12}) \ . \tag{A.7}$$

To calculate the determinant of R we need to solve the eigenvalue equation

$$(1-r_1)v_a + (r_1 - r_0)\sum_b \epsilon_{ab} v_b + (r_0 - q^2_{12})\sum_b v_b = \lambda v_a \ . \tag{A.8}$$

Let us distinguish three cases:

i) If

$$\sum_b \epsilon_{ab} v_b = 0 \qquad \forall \quad a \ , \tag{A.9}$$

and, consequently,

$$\sum_b v_b = 0 \ , \tag{A.10}$$

we have

$$\lambda_1 = (1 - r_1) \ . \tag{A.11}$$

In (A.9) the number of independent equations is equal to the number of blocks, that is m/x_r; the degeneration of the previous eigenvalue is then

$$d_1 = m - m/x_r \ . \tag{A.12}$$

ii) If

$$\sum_b v_b = 0 \ , \tag{A.13}$$

we obtain:

$$\lambda_2 = (1 - r_1) + x_r(r_1 - r_0) \ , \tag{A.14}$$

because the elements of the vector $\mathbf{v}$ must be equal in blocks of size x_r. The number of equations determining λ_2 is one and thus we have

$$d_2 = m - (m - m/x_r) - 1 = m/x_r - 1 \ . \tag{A.15}$$

iii) If the previous conditions are not satisfied, and the sums are all different from zero equation (A.8) gives

$$\lambda_3 = (1 - r_1) + x_r(r_1 - r_0) + m(r_0 - q_{12}^2) \ , \tag{A.16}$$

$$d_3 = 1 \ , \tag{A.17}$$

Expression (A.6) then becomes

$$\begin{aligned} \frac{1}{m} \log \det R = \log(1-r_1) + & \frac{1}{x_r} \log\left(1 + x_r \frac{r_1 - r_0}{1 - r_1}\right) \\ & + \frac{1}{m} \log\left(1 + m \frac{r_0 - q_{12}^2}{1 - r_1 + x_r(r_1 - r_0)}\right) \xrightarrow[m\to 0]{} \\ \log(1-r_1) + & \frac{1}{x_r} \log\left(1 + x_r \frac{r_1 - r_0}{1 - r_1}\right) + \frac{r_0 - q_{12}^2}{1 - r_1 + x_r(r_1 - r_0)} \ . \end{aligned} \tag{A.18}$$

From (A.2) and (A.18) we get the final form

$$\begin{aligned} -2\beta V_2(q_{12}) = & \ 2\beta^2 f(q_{12}) + \beta^2(x_r - 1) f(r_1) - \beta^2 x_r f(r_0) \\ & + \log(1 - r_1) + \frac{1}{x_r} \log\left(1 + x_r \frac{r_1 - r_0}{1 - r_1}\right) + \frac{r_0 - q_{12}^2}{1 - r_1 + x_r(r_1 - r_0)} \ . \end{aligned} \tag{A.19}$$

For the sake of completeness we note that there is a different method by which computing the potential, based on the formula

$$\begin{aligned} & -\beta N V_2(q_{12}) = \\ & = \lim_{n\to 0} \lim_{R\to 1} \frac{1}{n} \frac{\partial}{\partial R} \overline{\left(\int d\sigma \exp(-\beta H(\sigma)) \left(\int d\tau \exp(-\beta H(\tau)) \delta(q_{\sigma\tau} - q_{12}) \right)^{R-1} \right)^n} \\ & \qquad - \overline{\log Z_{free}} \ , \end{aligned} \tag{A.20}$$

where in the calculation of the average R has to be considered as an integer (compare with eq. (2.5)). In this way the replicated partition function takes the form

$$Z^{n,R} = \overline{\int d\tau_a^r \exp\left[-\beta \left(\sum_{a=1}^{n} \sum_{r=1}^{R} H(\tau_a^r) \right) \right] \prod_{a=1}^{n} \prod_{r=2}^{R} \delta(\tau_a^1 \tau_a^r - q_{12})} \ , \tag{A.21}$$

where we set $\sigma_a = \tau_a^1$. With this approach we obtain a $nR \times nR$ global overlap matrix $\mathbf{Q}$, formed by the $n \times n$ sub-matrices Q^{rs}_{ab} with $a, b = 1, \dots, n;\ r, s = 1, \dots, R$. In this way, the matrix Q^{11} encodes the overlap 1-1, the matrices Q^{1r} the overlap 1-2 and the matrices Q^{rs} with $r, s \neq 1$ encode the overlap 2-2. The ansatz that has to be taken for the various matrices is a mere translation in this context of the one exposed in Sect. 2.

The same line of reasoning can be applied in the computation of the three replica potential. Obvioulsy, in both cases, the two methods are equivalent.

Appendix B.

In this appendix we calculate the final form of the potential V_3. We have:

$$-\beta V_3(q_{12}, q_{13}, q_{23}) = \lim_{n,m,l\to 0} \frac{1}{2l}\left(\beta^2 \sum_{a,b} f(\mathbf{Q}_{ab}) + \log\det\mathbf{Q}\right) + \beta F_{free} \ . \tag{B.1}$$

The first part is

$$\begin{aligned}\lim_{n,m,l\to 0} \frac{1}{l}\beta^2 \sum_{ab} f(\mathbf{Q}_{ab}) =& 2\beta^2 f(q_{13}) + 2\beta^2 f(q_{23}) + 2\beta^2 (x_r - 1) f(w_{23}) - 2\beta^2 x_r f(z_{23}) \\ &+ \beta^2 f(1) + \beta^2 (x_s - 1) f(s_1) - \beta^2 x_s f(s_0) \ .\end{aligned} \tag{B.2}$$

For the second part we use the following relation:

$$\begin{aligned}&\log\det\mathbf{Q} = \\ &= \log\det Q^{11} \\ &+ \log\det[Q^{22} - Q^{21}(Q^{11})^{-1}Q^{12}] \\ &+ \log\det[Q^{33} - Q^{31}(Q^{11})^{-1}Q^{13} \\ &\quad - (Q^{23} - Q^{21}(Q^{11})^{-1}Q^{13})^T (Q^{22} - Q^{21}(Q^{11})^{-1}Q^{12})^{-1} (Q^{23} - Q^{21}(Q^{11})^{-1}Q^{13})] \ ,\end{aligned} \tag{B.3}$$

where we adopted the previous notation for the transposed matrices. The first two parts in the r.h.s reproduce the case of the two replicas potential and both go to zero when $(n, m, l) \to 0$.

The remaining parts of the determinant are:

$$
\begin{aligned}
Q^{31}(Q^{11})^{-1}Q^{13} &= q_{13}^2 \\
Q^{21}(Q^{11})^{-1}Q^{13} &= q_{12}q_{13} \\
Q^{21}(Q^{11})^{-1}Q^{12} &= q_{12}^2 \ ,
\end{aligned}
\tag{B.4}
$$

constant matrices. Finally, let us compute the inverse of $A = Q^{22} - q_{12}^2$:

$$
A_{ab} = (1-r_1)\delta_{ab} + (r_1 - r_0)\epsilon_{ab} + (r_0 - q_{12}^2) \ , \tag{B.5}
$$

that is,

$$
(A^{-1})_{ab} = \frac{1}{1-r_1}\ \delta_{ab} + \frac{r_0 - r_1}{1-r_1} \cdot \frac{1}{1 - r_1 + x_r(r_1 - r_0)}\ \epsilon_{ab} + \frac{q_{12}^2 - r_0}{(1 - r_1 + x_r(r_1 - r_0))^2} \ . \tag{B.6}
$$

Now it is possible to calculate the product

$$
\pi = (Q^{23} - Q^{21}(Q^{11})^{-1}Q^{13})^T (Q^{22} - Q^{21}(Q^{11})^{-1}Q^{12})^{-1} (Q^{23} - Q^{21}(Q^{11})^{-1}Q^{13}) \ . \tag{B.7}
$$

As can be easily seen the three matrices have the correct form, since they are RSB matrices with the same breaking point x_r. Due to this fact, the result of this product is a constant, although very complicate, given in eq. (3.11).

Now it remains to calculate:

$$
\log\det[Q^{33} - y] \ ; \tag{B.8}
$$

proceeding as in Appendix A, with y instead of q_{12}^2, we get

$$
\frac{1}{l}\log\det[Q^{33} - y] = \log(1 - s_1) + \frac{1}{x_s}\log\left(1 + x_s\frac{s_1 - s_0}{1 - s_1}\right) + \frac{s_0 - y}{1 - s_1 + x_s(s_1 - s_0)} \ . \tag{B.9}
$$

In this way we recover equation (3.10).

References.

[1] D.J. Thouless, P.W. Anderson, R.G. Palmer, *Philos. Mag.* **35** (1977), 593.

[2] J. Kurchan, G. Parisi, M.A. Virasoro, *J. Phys. I France* **3** (1993), 1819.

[3] A. Crisanti, H.J. Sommers, *J. Phys. I France* **5** (1995), 805.

[4] L.F. Cugliandolo, J. Kurchan, *Phys. Rev. Lett.* **71** (1993), 173.

[5] S. Franz, G. Parisi, *J. Phys. I France* **5** (1995), 1401.

[6] D.J. Gross, M. Mézard, *Nucl. Phys. B* **240** (1984), 431.

[7] E. Gardner, *Nucl. Phys. B* **257** (1985), 747.

[8] T.R. Kirkpatrick, D. Thirumalai, *Phis. Rev.* B **36** (1987), 5388.

[9] A. Crisanti, H.J. Sommers, *Z. Phys.* B **87** (1992), 341.

[10] M. Mézard, G. Parisi, *J. Phys. A* **23** (1990), L1229; *J. Phys. I France* **1** (1991), 809.

[11] Th.M. Nieuwenhuizen, *Phys. Rev. Lett.* **74** (1996), 4289.

[12] S. Franz, private communication.

[13] A. Barrat, R. Burioni, M. Mézard, *J. Phys* A **29** (1996), L81.

[14] M.A.Virasoro, *Simulated annealing methods under analytical control*, in Proceedings of 19th Intl. Conf. on Stat. Phys. (IUPAP), Xiamen, China; to be published.

[15] M.E. Ferrero, M.A. Virasoro, *J. Phys. I France* **4** (1994), 1819.